Quenching rattling modes in skutterudites with pressure

I. Sergueev, K. Glazyrin, I. Kantor, M. A. McGuire, A. I. Chumakov, B. Klobes, B. C. Sales, and R. P. Hermann

Phys. Rev. B **91**, 224304 — Published 15 June 2015

DOI: 10.1103/PhysRevB.91.224304

Quenching "rattlers" in Skutterudites with Pressure

I. Sergueev,[1,*] K. Glazyrin,[1] I. Kantor,[2] M. A. McGuire,[3] A. I. Chumakov,[2] B. Klobes,[4] B. C. Sales,[3] and R. P. Hermann[4,5]

[1]*Deutsches Elektronen-Synchrotron, D-22607 Hamburg, Germany*

[2]*European Synchrotron Radiation Facility (ESRF), P.O. Box 220, F-38043 Grenoble, France*

[3]*Materials Science and Technology Division, Oak Ridge National Laboratory, Oak Ridge, Tennessee 37831, USA*

[4]*Jülich Center for Neutron Science JCNS and Peter Grünberg Institut PGI, JARA-FIT, Forschungszentrum Jülich GmbH, D-52425 Jülich, Germany*

[5]*Faculté des Sciences, Université de Liège, B-4000 Liège, Belgium*

(Dated: May 18, 2015)

Abstract

A high-pressure study of the lattice dynamics in the filled skutterudite $Eu_{0.84}Fe_4Sb_{12}$ was carried out by means of X-ray powder diffraction and nuclear inelastic scattering. The anharmonicity of particular phonon modes was characterized by mode and element specific Grüneisen parameters. The large anharmonicity of the "rattling" optical mode that is hybridized with the acoustical phonons at ambient pressure is reduced at high pressure as the phonon modes decouple. This result suggests that anharmonic coupling between acoustic and optical phonon modes plays a central role in the reduced thermal conductivity.

I. INTRODUCTION

The growing demand for sustainable energy and efficient heat-to-electricity conversion stimulates the search for novel thermoelectric materials. Starting from the mid-1990s, the focus of thermoelectric research shifted from conventional materials such as PbTe and Bi_2Te_3 to materials with more complex structures[1,2] or with tailored nanostructures[3]. The exploration of materials with structures containing large voids that accommodate loosely bound "rattling" atoms, such as filled skutterudites and clathrates is one promising avenue. The idea that such "rattling" atoms would strongly scatter the propagating acoustic phonons[4,5] and, thus, decrease the thermal conductivity was experimentally verified for $CeFe_4Sb_{12}$, $LaFe_3CoSb_{12}$, and $(Sr,Eu)_8Ge_{16}Si_{30}$[6–8] among other compounds. Surprisingly, even after 20 years of intensive research the microscopic mechanism behind the reduced thermal conductivity in filled skutterudites and clathrates remains unclear and debated. The original simple picture of non-correlated motion[5] of the "rattling" atoms, independent of the host structure, has gradually been challenged and refined by inelastic neutron and nuclear inelastic scattering[9–11] and by theoretical calculations[12,13]. A strongly anharmonic interatomic potential for the "rattling" atoms was suggested[14] as origin of the reduced thermal conductivity, and this hypothesis correlates with experimental results[15]. Other models explain the low thermal conductivity in the filled compounds by enhanced Umklapp scattering[16] or modification of the phonon dispersions without increase of the anharmonicity[17]. Hybridization of the "rattling" optical mode and the acoustical modes has been observed for several filled skutterudites[9,18] and clathrates[19]. Theoretical investigations suggest that highly anharmonic hybridization between the localized "rattling" mode and the acoustical modes leads to scattering of the acoustical phonons and reduced thermal conductivity[20]. An experimental verification of this idea was, however, still lacking mainly due to the difficulties in measuring mode specific anharmonicity.

The anharmonic contribution to the interatomic potential can be quantified by the phonon mode specific Grüneisen parameters $\gamma_i = -\partial \ln E_i / \partial \ln V$ that relate the change in the phonon mode energy (E_i) upon volume (V) change of the material. By definition, measurement of the mode specific Grüneisen parameter requires observation of phonon mode shifts as a function of volume change in response to a variation of pressure or temperature. Investigation of the "rattling" and other optical phonon modes' evolution with pressure was done

by Raman scattering in chlatrates[21–23] a method that does not work in filled skutterudites as the "rattling" mode is not Raman active.

Here, we report the measurements of the lattice dynamics as a function of pressure in the filled skutterudite $Eu_{0.84}Fe_4Sb_{12}$ by nuclear inelastic scattering (NIS)[24], a technique which through its element selectivity provides partial densities of phonon states (PDOS) individually for the guest atoms and for the host structure. A combination of these PDOS with density information obtained from the high pressure powder X-ray diffraction yields element specific Grüneisen parameters for a set of individual phonon modes. A large Grüneisen parameter was found for the "rattling" mode which is hybridized with the acoustical phonons at ambient and moderate pressure. At critical pressure of ∼12 GPa the Grüneisen parameter for the "rattling" mode is reduced and phonon modes decouple. This result supports the hypothesis that anharmonic coupling between acoustic and optical phonon modes plays a central role in the reduced thermal conductivity in filled skutterudites.

II. MATERIALS AND METHODS

A. Sample preparation and characterization

^{57}Fe powder from Cambridge Isotopes was reduced in flowing H_2 gas (3.5%, balance Ar) at 800 C for 12 hours. The reduced powder was combined with elemental Eu and Sb pieces in the stoichiometric ratios Eu:Fe:Sb = 1:4:12 inside a glovebox, after cleaning the surface of the Eu metal with a wire brush. The mixture was placed in an carbon coated silica glass crucible and sealed inside a silica glass ampoule. The material was melted at 1000 C for 2 hours and quenched in ice water. The boule was then annealed at 700 C for 4 days and quenched in ice water. Rietveld refinement of powder x-ray diffraction revealed the sample to be nearly single phase skutterudite with composition $Eu_{0.84}Fe_4Sb_{12}$, with less than 1 wt.% Sb as the only detected impurity. Careful exclusion of oxygen, especially from the iron powder, was crucial to avoiding formation of high levels of impurity phases. Mössbauer spectral analysis of the samples with the ^{151}Eu, ^{121}Sb, and ^{57}Fe nuclear resonances indicate no foreign phases, at a 1% detection limit.

B. Experimental methods

NIS measurements were performed at the nuclear resonance beam line ID18[25] at the European Synchrotron Radiation Facility with the ^{151}Eu, ^{57}Fe, and ^{121}Sb nuclear resonances. High resolution monochromators provided energy bandwidths of 0.7 meV at 14.4 keV, 1.1 meV at 21.5 keV, and 1.2 meV at 37.1 keV for the nuclear resonances of the ^{57}Fe, ^{151}Eu, and ^{121}Sb isotopes, respectively. The high pressure ^{151}Eu and ^{57}Fe NIS measurements were performed using powder samples loaded into the diamond anvil cell (DAC) with paraffin as a pressure medium. The ^{121}Sb NIS measurements were not conducted at high pressure because the low Lamb-Mössbauer factor at room temperature leads to blurring of the NIS spectrum by multiphonon contributions. The individual ^{151}Eu and ^{57}Fe NIS measurements were performed using the same DAC, on the same sample and after stabilization of the desired pressure. Pressure was measured using ruby spheres loaded into the DAC gasket chamber in the vicinity of the sample material. The choice of paraffin as a pressure medium was dictated by our requirements to have a good quasi-hydrostatic pressure medium.

The ^{151}Eu nuclear forward scattering (NFS) was carried out together with NIS in order to measure the isomer shift of Eu in $Eu_{0.84}Fe_4Sb_{12}$ against Eu_2O_3 at high pressure. The $Eu_{0.84}Fe_4Sb_{12}$ sample in DAC and Eu_2O_3 target were installed into the X-ray beam and time spectra were measured at 296 K

The high pressure X-ray diffraction was conducted at the beamline P02.2[26] at the PETRAIII X-ray light source at 42.8 keV X-ray energy with the beam size of 2×2 μm^2 on material taken from the same synthesis batch loaded into a symmetric Mao-type DACs. In compliance with NIS studies paraffin was used as a pressure medium and pressure was measured using ruby spheres.

C. Data treatment

The partial densities of phonon states (PDOS) were evaluated from the NIS spectra using the procedure described in Ref. 27. No deconvolution with the instrumental function was applied, so that the statistical noise in the PDOS reproduces that in the NIS spectra. The extraction of the Fe PDOS works well which is confirmed by deviation of the PDOS area from unity by less than 1%. The evaluation of the Eu PDOS is more difficult due to the small

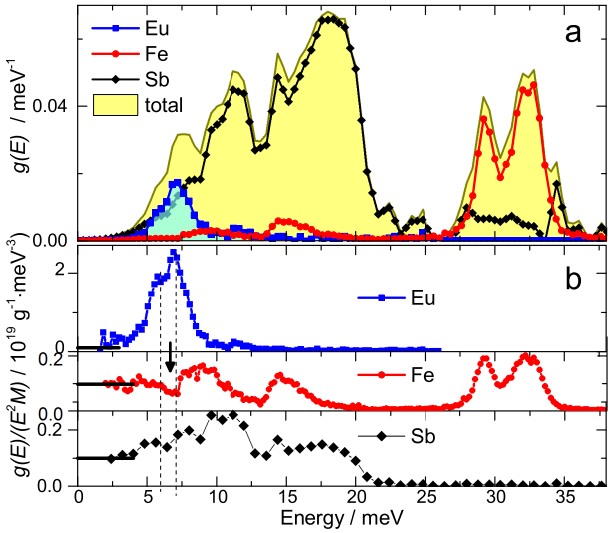

FIG. 1: (a) Element specific and total density of phonon states, $g(E)$, of $Eu_{0.84}Fe_4Sb_{12}$ measured at 40 K. (b) the corresponding reduced partial density of phonon states $g(E)/(E^2M)$ scaled by the atomic mass. The thick horizontal lines show the Debye level, $1/(2\pi^2\hbar^3\rho\langle v\rangle^3)$, obtained from the Fe PDOS where ρ is the density and $\langle v\rangle$ is the mean sound velocity of the material. The dashed vertical lines emphasize the region of the "rattling" peak. The arrow emphasizes the dip in the Fe reduced PDOS.

Lamb-Mössbauer factor at 296 K, which is 0.18 at ambient pressure and 0.35 at 20.3 GPa. This leads to a large multiphonon contribution in the spectrum which is difficult to take into account correctly. The multiphonon parts add smooth pedestal to the spectra[28]. Thus, the obtained PDOS can have incorrect slowly changed background which manifests itself in the deviation of the obtained PDOS area from unity by up to 10%. However, this contribution does not affect the sharp features, in particular the position and width of the peaks, which allows us to extract position of the peaks.

III. RESULTS AND DISCUSSION

A. Ambient pressure

The $Eu_{0.84}Fe_4Sb_{12}$ compound is representative of the filled antimony skutterudites, RM_4Sb_{12}, where R is a rare earth and M is a transition metal. This composition is particularly appealing because it displays rattling behavior and NIS measurements can be carried out using nuclear resonances from all three constituent atoms, ^{151}Eu, ^{57}Fe, and ^{121}Sb.

Figure 1(a) shows the PDOS, $g(E)$, for Fe, Eu, and Sb derived[27] from the NIS spectra

measured at 40 K and ambient pressure. The shapes of the obtained PDOS are in good agreement with previous measurements[10,11] and also agree with the calculations for similar compound $LaFe_4Sb_{12}$[13]. The PDOS of the guest Eu features a well pronounced slightly split "rattling" peak at 7 meV and small peak at 11.5 meV which coincides with the position of the pronounced peak in the PDOS for Sb. The vibrations of the Sb and Fe are occurred mainly at 5-20 and 27-35 meV, respectively.

The interesting features are observed at low energies and around the "rattling" peak of Eu at 7 meV. They are seen in the reduced PDOS, $g(E)/(E^2M)$,where M is the mass of the corresponding element, in Fig. 1(b). The Debye-like behavior for the low-energy acoustical modes, for which all atoms vibrate in phase, leads to a unique constant for this function[24] related solely to the speed of sound and density, as indeed is observed below 5 meV. Around 7 meV, the reduced PDOS of Eu reveals a split peak, whereas the reduced PDOS of Fe shows a pronounced dip indicated by arrow. A similar dip in the reduced Fe PDOS at position of the "rattling" peak was observed in $YbFe_4Sb_{12}$[29] and La(Pr,Sm)Fe_4Sb_{12}[30]. This dip does not appear in the unfilled skutterudite $FeSb_3$[29]. The presence of the dip in the reduced Fe PDOS at position of the "rattling" peak as well as a Eu peak at about 11 meV, i.e., at the position of the pronounced peak in the Sb PDOS show that the motion of the guest Eu coupled to the framework formed by Fe and Sb, in line with conclusions of Ref. 9. As we show below, both the split structure of the peak in the PDOS for Eu and the pronounced dip in the PDOS for Fe are the manifestation of the "avoided crossing" hybridization of the "rattling" optical and propagating acoustic modes.

The hybridization of the acoustic and Einstein-like optical phonon modes can be considered using a simple one-dimensional spring model[19]. The main results of these models are illustrated by Fig. 2. For a weak coupling between the host and guest atoms, the dispersion relations exhibit an "avoided crossing" (Fig. 2(a)). This behavior of the dispersion relations leads to the split peak in the PDOS of the model guest and the dip in the PDOS of the model host atoms. This is exactly what is observed in our measurements: the split peak in the reduced PDOS for the guest Eu and the pronounced dip in the reduced PDOS of the host Fe (Fig. 1(b)). As far as Sb is concerned, we note that in the crystal lattice they occupy the intermediate positions between Eu and Fe. Thus, the reduced PDOS of Sb around the "rattling" peak shows the trend intermediate between that for the Eu and Fe as seen in Fig. 1(b). This observation indicates that the phonon dispersion relations in the vicinity of

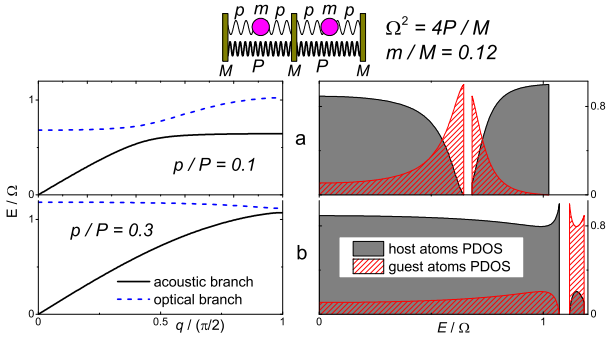

FIG. 2: Simple one dimensional spring model (top) describing interactions between hosts of mass M and interconnected with a spring constant P with guests mass m attached to the hosts with a spring constant p. Here the guest and host represent Eu and Fe, respectively, of $Eu_{0.84}Fe_4Sb_{12}$. Bottom: phonon dispersion relations (left) and PDOS (right) calculated for different ratios of the coupling, p/P. "Avoided crossing" hybridization between acoustical and optical branches occurs at (a) whereas the conventional order of acoustical and optical phonon branches is seen in (b). The one-dimensional PDOS corresponds to the reduced PDOS in three dimensions for geometrical reasons.

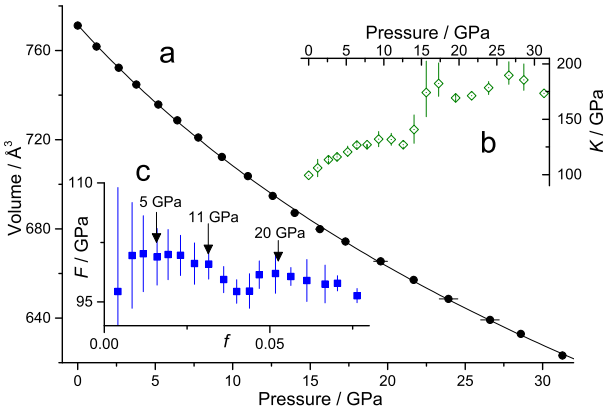

FIG. 3: (a) Pressure dependence of the unit cell volume of $Eu_{0.84}Fe_4Sb_{12}$. The line is Birch-Murchagan equation of state fit. (b) Bulk modulus K vs pressure. (c) Normalized pressure, F, vs Eulerian strain f.

the "rattling" peak are described by the "avoided crossing" hybridization of the acoustical and "rattling" optical modes.

B. High pressure

Three types of measurements were conducted at room temperature and pressures up to 20 GPa: the high pressure X-ray powder diffraction, the ^{151}Eu nuclear forward scattering and the ^{57}Fe and ^{151}Eu nuclear inelastic scattering.

The pressure dependence of the $Eu_{0.84}Fe_4Sb_{12}$ unit cell volume is shown in Fig. 3. The material maintains the same structure in the full pressure range of our study. The data were fitted by the 3rd order Birch-Murchagan equation of states[31] resulting in the following fit parameters: $V_0 = 771.4(9)$ A^3, $K_0 = 100(2)$ GPa, and $K_0' = 3.6(2)$, where V_0 is the volume, K_0 is the bulk modulus and K_0' is the bulk modulus pressure derivative at ambient conditions.

The isomer shift of Eu in $Eu_{0.84}Fe_4Sb_{12}$ at high pressure was obtained by NFS. The NFS intensity of $Eu_{0.84}Fe_4Sb_{12}$ at different pressures and Eu_2O_3 calibrated target is shown in Fig. 4. The intensity, $I(t)$, was fitted by equation:

$$E(t) = \mathrm{e}^{-at/2\tau_0} + k \cdot \mathrm{e}^{(-b+2i\Omega)/2\tau_0} \quad (1)$$

$$I(t) = I_0 \cdot |E(t - t_0)|^2 \quad (2)$$

where Ω is the isomer shift of $Eu_{0.84}Fe_4Sb_{12}$ relative to Eu_2O_3 , a and b are the line widths for two samples, τ_0 is the natural lifetime (τ_0=14.0 ns), k is the ratio of the line areas. I_0 and t_0 account for the total intensity and shift of the zero time. The obtained relative isomer shift is shown in Fig. 4 . The shift of 11 - 11.8 mm/s relative to trivalent Eu in Eu_2O_3 is observed for Eu in $Eu_{0.84}Fe_4Sb_{12}$. The similar relative isomer shift (11.8 mm/s) versus Eu_2O_3 was observed[32] for EuS. Typically, the divalent Eu compounds have isomer shift of about (-11:-14) mm/s relative to the trivalent EuF_3 and less precisely to Eu_2O_3[33]. Thus, the Eu in $Eu_{0.84}Fe_4Sb_{12}$ remains divalent up to 20 GPa.

The evolution of the Fe and Eu NIS spectra versus applied pressure, shown in Fig. 5, demonstrates the expected phonon mode hardening without significant change in shape. An enhanced hardening rate of the Eu "rattling" peak is clearly visible when compared to the position of the neighboring Fe peak located at ∼8 meV. Whereas these peaks are separated at ambient pressure, they strongly overlap already at 10.1 GPa. In addition, the Fe inelastic spectrum features a peculiar evolution: the dip present at ambient conditions at the position of the 7 meV "rattling" Eu mode disappears above 10.1 GPa.

The Fe and Eu PDOS obtained from the data are shown in the Fig. 6. The obtained values of the Lamb-Mössbauer factor, the atomic displacement parameters and the mean force constants are presented in the Table I.

The relative energy shift of specific peaks of the Fe and Eu NIS spectra and PDOS were

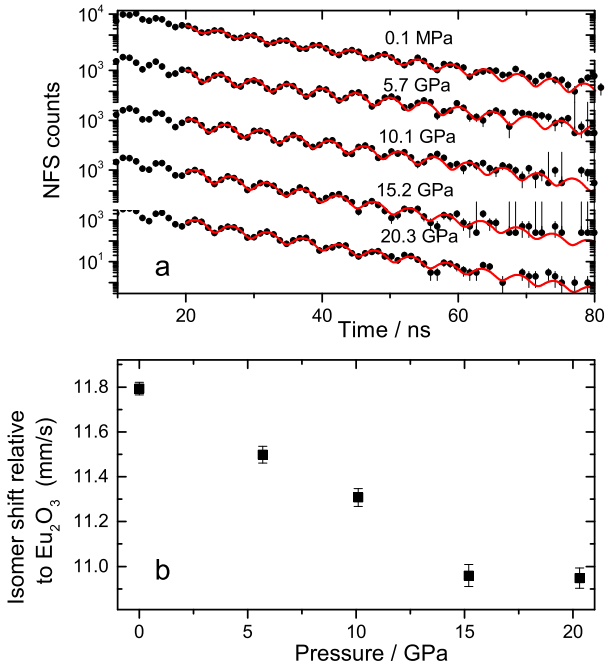

FIG. 4: (a): NFS spectra for of $Eu_{0.84}Fe_4Sb_{12}$ and Eu_2O_3 measured at different pressures and 296 K. The lines show fit according to equation. (b): isomer shift of Eu in $Eu_{0.84}Fe_4Sb_{12}$ relative to Eu_2O_3 as a function of pressure.

TABLE I: The Lamb-Mössbauer factors f_{LM}, atomic displacement parameters U_{eq}, mean force constants Φ and Debye energy E_D in $Eu_{0.84}Fe_4Sb_{12}$ at different temperatures and pressures.

Element	P(GPa)	T(K)	f_{LM}	U_{eq}(Å^2)	Φ (N/m)	E_D (meV)
Fe	amb	47	0.915(1)	0.00167(2)	187(2)	31.9(6)
Eu	amb	36	0.74(1)	0.00254(10)	44(5)	
Sb	amb	45	0.60(2)	0.00146(10)	148(5)	
Fe	amb	296	0.763(1)	0.00509(2)	182(2)	30.8(1)
Fe	5.7	296	0.772(1)	0.00485(2)	215(2)	31.5(4)
Fe	10.1	296	0.791(1)	0.00439(2)	245(2)	32.7(4)
Fe	15.2	296	0.800(1)	0.00418(2)	277(2)	33.1(4)
Fe	20.3	296	0.799(1)	0.00421(2)	294(2)	32.7(5)
Eu	amb	296	0.18(2)	0.0146(10)		
Eu	5.7	296	0.26(2)	0.0115(6)		
Eu	10.1	296	0.31(2)	0.0099(5)		
Eu	15.2	296	0.34(2)	0.0091(5)	78(5)	
Eu	20.3	296	0.35(2)	0.0088(5)	76(5)	

obtained using the procedure described in Ref. 34. The NIS spectrum and PDOS with the best statistics (ambient pressure, 296 K) were used as a theoretical function $D(E)$ via linear interpolation of the data. All other data sets were fitted in the regions of the peak of interest by the function $b \cdot D((1+a) \cdot E)$, where a and b are fit parameters. The parameter a gives

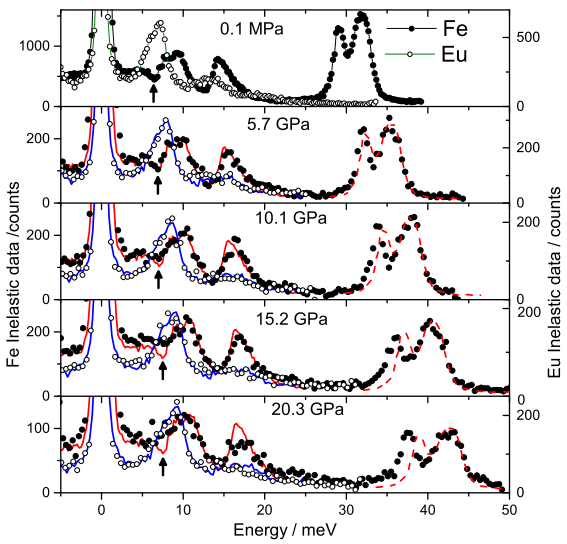

FIG. 5: Eu and Fe inelastic spectra in $Eu_{0.84}Fe_4Sb_{12}$ measured at different pressures. The solid lines show ambient pressure data scaled in energy in order to match the Eu 7 meV peak (blue line) and the Fe 9 meV (red solid line) and 32 meV (red dash line) peaks. The arrows point out position of the dip in the Fe spectra pronounced below 10 GPa and disappeared above.

the shift of the peak position $a = \Delta E/E_0$ relative to the position in the reference data set. Such procedure was applied for characteristic Fe peaks at 9, 14, 29, and 32 meV and for Eu peak at 7 meV. The quality of the fit are shown in the Fig. 6 for PDOS peaks and in the Fig. 5 for the peaks in the NIS spectra. The fit of both spectra and PDOS give consistent results and the error were taken as a maximum error between these two fits. The parameters a obtained from the fit are presented in the Supplemental part. The Eu 11 meV peak was fitted only in PDOS with the same procedure where Eu PDOS at ambient pressure, 40 K is taken as the theoretical function. The shift of this peak between 40 and 296 K is estimated and included into the total error for the relative energy shift.

The Debye energy was obtained from the reduced Fe PDOS, $g(E)/E^2$, by fit in the range 2.4-5.2 meV with constant parameter $\alpha = 3/E_D^3$. The Fe PDOS above 2.4 meV is not affected by subtraction of the elastic line. The obtained values Debye energy are presented in Table I.

The relative shift of particular phonon modes, $\Delta E/E_0$, as a function of the volume contraction, $\Delta V/V_0$ is shown in Fig. 7. Contrasting behavior is observed for the Fe modes on one hand and the Eu and acoustical modes on the other hand. The Fe optical modes starting from the peak at 9 meV harden linearly, whereas a kink is observed at 12-13 GPa

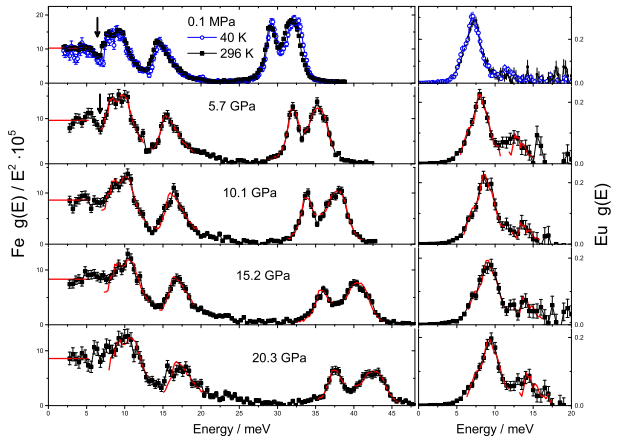

FIG. 6: Left: Fe reduced PDOS, $g(E)/E^2$ for different pressures. The red horizontal line at low energy show fit of the Debye level, the red segment lines show fit of high pressure data by the reference PDOS. The arrows show presence of the dip in the Fe reduced PDOS at 5.7 and 10.1 GPa. Right: Eu PDOS, $g(E)$, for different pressures. The red segment lines are the fit by the reference PDOS.

for the Eu modes and the Debye energy, i.e. acoustical modes. Fits of the data by linear functions yield the Grüneisen parameters shown in Fig.7(b) and 7(c), below and above 10.1 GPa, respectively. In the low pressure region, the Grüneisen parameters for the Fe modes increase with phonon energy from 0.6 for the acoustical phonons up to 2.3 for the optical modes near 33 meV. The Eu modes Grüneisen parameters deviate from this trend: the "rattling" mode located at 7 meV at ambient pressure has $\gamma = 2.5$ which is 2 times larger than the Grüneisen parameter for the Fe modes with comparable energies, a deviation that reveals an enhanced anharmonicity of the interatomic potential of the Eu guests. The Grüneisen parameters obtained here are in good agreement with the calculations for the filled skutterudite $LaFe_4Sb_{12}$[20,35] which also predicts large γ value for the "rattling" mode.

Above 10.1 GPa, the Grüneisen parameters drastically change: the enhanced γ for the Eu modes is reduced, and all modes between 5 and 20 meV have comparable γ. In addition, the averaged acoustical mode Grüneisen parameter obtained from the Debye energy is strongly decreased, $\gamma = 0.02(20)$. All these features correspond to the theoretical calculations of γ for the unfilled skutterudite[20]. Thus, the evolution of the lattice dynamics with pressure suggests the presence of a transition at a critical pressure around 10 GPa where the anharmonicity of the interatomic potential is suppressed for the "rattling" mode. The existence of this transition in which essentially the "rattling" is switched off has never been observed or predicted before.

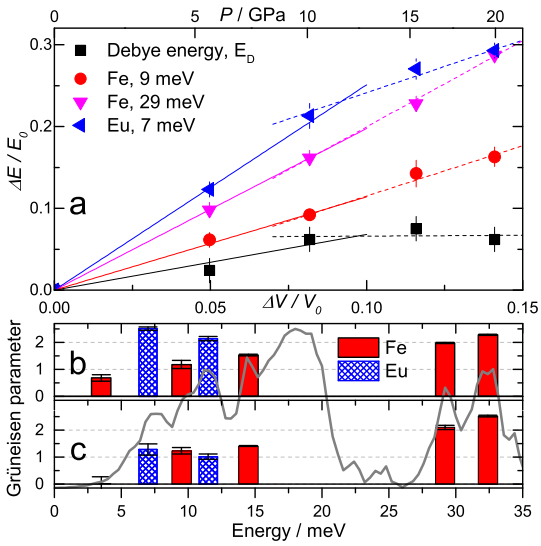

FIG. 7: (a) Dependence of the relative energy of particular phonon modes upon relative volume contraction. The solid and dashed lines show linear fits in the 0-10 and 10-20 GPa regions, respectively. The Grüneisen parameters of the modes obtained as a linear slope parameter of the fits are shown in (b) and (c) for pressures below and above 10 GPa, respectively. The gray line in (b) and (c) reproduces the total DOS of Fig. 1.

The suppression of hybridization of the optical "rattling" mode and the acoustical modes, which leads to the transformation from "avoided crossing"-type phonon dispersion relations to dispersion relations where the "rattling" optical modes shifts above the acoustical modes appears to be the origin of this transition. This scenario is illustrated in the one-dimensional spring model in Fig. 2. The increase of the host-guest coupling leads to strong hardening of the optical mode and to the transition described above. The characteristic feature of the transition in this model is the disappearance of the dip in the low-energy part of the host PDOS, as is observed in the Fe inelastic spectra around 10.1 GPa.

In contrast to the ball-and-spring model where the transition is introduced by increasing the host-guest coupling artificially in a harmonic vibrational model, in the real system, this increase of the coupling comes from the anharmonicity of the guest interatomic potential. The quenching of the anharmonicity above the transition is a central result: it suggests that there is a connection between the "avoided crossing" hybridization between the acoustical and optical "rattling" phonon modes and the anharmonicity of these modes.

A further test of the change in Grüneisen parameter of the acoustical modes with a critical pressure around 10 GPa comes from the bulk compressibility ($K = -V[dP/dV]$), the elastic

property directly related to longitudinal sound propagation in the material. The change of the Grüneisen parameter of the Debye energy, E_D, suggests a jump in the derivative of the sound velocity and, subsequently, may produce a jump in the pressure derivative of the bulk modulus, K'[36]. A detailed analysis of the diffraction data reveals an anomaly in the bulk compressibility around 12-18 GPa, see Fig. 7(b). The same anomaly is seen from the analysis of the stress-strain relation in a so-called $F - f$ plot shown in Fig. 7(c) which relates the variation of normalized stress $F = P/[3f(1 + 2f)^{5/2}]$ with the Eulerian strain $f(V) = [(V_0/V)^{2/3} - 1]/2$[36]. A change in the F slope in indicates a discontinuity in the bulk compressibility, K, or its derivative, K'[37]. Such anomaly is visible in our data between 12 and 18 GPa.

Thus, the analysis of both the structural and lattice dynamics data indicates the existence of the critical pressure around 12 GPa where the decoupling of the acoustic and "rattling" modes modifies the elastic properties of the material. Similar features are thus expected in the compressibility data for other filled skutterudites. In the only report so far in the pressure range above 10 GPa anomalous compressional behavior is observed in $CeFe_4Sb_{12}$ and $Ce_{0.8}Fe_3CoSb_{12}$ around 10-12 GPa[38] which is supplemented by slight slope change of the shear velocity and anomalies of the transport properties at 12 GPa in $Ce_{0.8}Fe_3CoSb_{12}$[39]. The suggested presence of an electronic topological transition due to the valence variation of the rare earth[39] is not supported by our results since we observe divalent Eu up to 20 GPa. Rather, we propose that these anomalies are explained by the decoupling of the phonon modes at a critical pressure which is present for the entire family of the filled skutterudites.

IV. CONCLUSION

In summary, the pressure dependence of the lattice dynamics in the filled skutterudite $Eu_{0.84}Fe_4Sb_{12}$, as studied by NIS and XRD yields element specific Grüneisen parameters and their variation under compression. Detailed analysis reveals the hybridization of the Eu "rattling" mode and acoustical modes at ambient pressure. At moderate pressure, up to 10 GPa, the Grüneisen parameters obtained for the Eu modes are indicative of a large anharmonicity of the interatomic potential for the Eu guests. Above the critical pressure of $\sim$12 GPa, both the hybridization of the modes and the enhanced anharmonicity disappear. This critical pressure coincides with a jump in the bulk compressibility and an anomaly

in the behavior of normalized stress as a function of Eulerian strain. We suggest that this anomaly in the vicinity of 12 GPa is caused by a decoupling and a subsequent reconstruction of the "rattling" and acoustical phonon modes. This decoupling leads to a reduction of the anharmonicity of the potential for the guests. Thus, it appears that at low pressure it is the hybridization of the acoustic phonon modes with the "rattling" optical mode that leads to the enhanced anharmonicity. Furthermore, our study predicts that the lattice thermal conductivity of the filled and unfilled skutterudites may become comparable at high pressure.

Acknowledgments

The European Synchrotron Radiation Facility and PETRA III X-ray light source are acknowledged for provision of synchrotron radiation beam time and facilities at beam lines ID18 and P02.2. Sample synthesis and characterization at Oak Ridge National Laboratory was supported by the US Department of Energy, Office of Science, Basic Energy Sciences, Materials Sciences and Engineering Division. The DFG priority program SPP1386 "Nanostructured Thermoelectrics" and the Helmholtz Association grant VH NG-407 are acknowledged for funding parts of this research.

---

* Electronic address: ilya.sergeev@desy.de

[1] G. J. Snyder and E. S. Toberer, Nature Materials **7**, 105 (2008).

[2] E. S. Toberer, L. L. Baranowski, and C. Dames, Annual Review of Materials Research **42**, 179 (2012).

[3] C. J. Vineis, A. Shakouri, A. Majumdar, and M. G. Kanatzidis, Advanced Materials **22**, 3970 (2010).

[4] G. A. Slack and V. G. Tsoukala, Journal of Applied Physics **76**, 1665 (1994), ISSN 0021-8979, 1089-7550.

[5] G. Slack, in *CRC Handbook of Thermoelectrics*, edited by D. Rowe (CRC Press, 1995), ISBN 978-0-8493-0146-9, 978-1-4200-4971-8.

[6] B. C. Sales, D. Mandrus, and R. K. Williams, Science **272**, 1325 (1996), ISSN 0036-8075, 1095-9203.

[7] B. C. Sales, D. Mandrus, B. C. Chakoumakos, V. Keppens, and J. R. Thompson, Physical Review B **56**, 15081 (1997).

[8] J. L. Cohn, G. S. Nolas, V. Fessatidis, T. H. Metcalf, and G. A. Slack, Physical Review Letters **82**, 779 (1999).

[9] M. M. Koza, M. R. Johnson, R. Viennois, H. Mutka, L. Girard, and D. Ravot, Nature Materials **7**, 805 (2008).

[10] H. C. Wille, R. P. Hermann, I. Sergueev, O. Leupold, P. van der Linden, B. C. Sales, F. Grandjean, G. J. Long, R. Rüffer, and Y. V. Shvyd'ko, Physical Review B **76** (2007), ISSN 1098-0121.

[11] G. J. Long, R. P. Hermann, F. Grandjean, E. E. Alp, W. Sturhahn, C. E. Johnson, D. E. Brown, O. Leupold, and R. Rüffer, Physical Review B **71**, 140302 (2005).

[12] J. L. Feldman, D. J. Singh, I. I. Mazin, D. Mandrus, and B. C. Sales, Phys. Rev. B **61**, R9209 (2000).

[13] J. L. Feldman, P. Dai, T. Enck, B. C. Sales, D. Mandrus, and D. J. Singh, Phys. Rev. B **73**, 014306 (2006).

[14] A. Yamakage and Y. Kuramoto, Journal of the Physical Society of Japan **78**, 064602 (2009), ISSN 0031-9015, 1347-4073.

[15] K. Iwasa, M. Kohgi, H. Sugawara, and H. Sato, Physica B: Condensed Matter **378-380**, 194 (2006), ISSN 0921-4526.

[16] C. H. Lee, I. Hase, H. Sugawara, H. Yoshizawa, and H. Sato, Journal of the Physical Society of Japan **75**, 123602 (2006).

[17] W. Li and N. Mingo, Phys. Rev. B **89**, 184304 (2014), URL `http://link.aps.org/doi/10.1103/PhysRevB.89.184304`.

[18] M. M. Koza, A. Leithe-Jasper, H. Rosner, W. Schnelle, H. Mutka, M. R. Johnson, M. Krisch, L. Capogna, and Y. Grin, Phys. Rev. B **84**, 014306 (2011).

[19] M. Christensen, A. B. Abrahamsen, N. B. Christensen, F. Juranyi, N. H. Andersen, K. Lefmann, J. Andreasson, C. R. H. Bahl, and B. B. Iversen, Nat Mater **7**, 811 (2008), ISSN 1476-1122.

[20] N. Bernstein, J. L. Feldman, and D. J. Singh, Phys. Rev. B **81**, 134301 (2010).

[21] J. S. Tse, S. Desgreniers, Z.-q. Li, M. R. Ferguson, and Y. Kawazoe, Phys. Rev. Lett. **89**, 195507 (2002).

[22] T. Kume, H. Fukuoka, T. Koda, S. Sasaki, H. Shimizu, and S. Yamanaka, Phys. Rev. Lett. **90**, 155503 (2003).

[23] T. Kume, S. Ohno, S. Sasaki, H. Shimizu, Y. Ohishi, N. L. Okamoto, K. Kishida, K. Tanaka, and H. Inui, Journal of Applied Physics **107**, 013517 (2010).

[24] A. Chumakov and R. Rüffer, Hyperfine Interactions **113**, 59 (1998).

[25] R. Rüffer and A. I. Chumakov, Hyperfine Interactions **97-98**, 589 (1996).

[26] H.-P. Liermann, W. Morgenroth, A. Ehnes, A. Berghäuser, B. Winkler, H. Franz, and E. Weckert, Journal of Physics: Conference Series **215**, 012029 (2010).

[27] V. Kohn and A. Chumakov, Hyperfine Interactions **125**, 205 (2000).

[28] A. Chumakov and W. Sturhahn, Hyperfine Interactions **123-124**, 781 (1999).

[29] A. Möchel, I. Sergueev, H.-C. Wille, J. Voigt, M. Prager, M. B. Stone, B. C. Sales, Z. Guguchia, A. Shengelaya, V. Keppens, et al., Phys. Rev. B **84**, 184306 (2011).

[30] S. Tsutsui, J. Umemura, H. Kobayashi, T. Tazaki, S. Nasu, Y. Kobayashi, Y. Yoda, H. Onodera, H. Sugawara, T. Matsuda, et al., Hyperfine Interactions **168**, 1073 (2006).

[31] F. Birch, Physical Review **71**, 809 (1947).

[32] O. Leupold, A. Chumakov, E. Alp, W. Sturhahn, and A. Baron, Hyperfine Interactions **123-124**, 611 (1999).

[33] F. Grandjean and G. Long, in *Mössbauer Spectroscopy Applied to Inorganic Chemistry*, edited by G. Long and F. Grandjean (Springer US, 1989), vol. 3 of *Modern Inorganic Chemistry*, pp. 513–597, ISBN 978-1-4899-2291-5.

[34] I. Sergueev, R. P. Hermann, D. Bessas, U. Pelzer, M. Angst, W. Schweika, M. A. McGuire, A. S. Sefat, B. C. Sales, D. Mandrus, et al., Physical Review B **87**, 064302 (2013).

[35] J. L. Feldman, D. J. Singh, and N. Bernstein, Physical Review B **89**, 224304 (2014).

[36] F. Birch, Journal of Geophysical Research: Solid Earth **83**, 1257 (1978), ISSN 2156-2202.

[37] B. J. Maier, A.-M. Welsch, B. Mihailova, R. J. Angel, J. Zhao, C. Paulmann, J. M. Engel, W. G. Marshall, M. Gospodinov, D. Petrova, et al., Physical Review B **83**, 134106 (2011).

[38] W. Liu, Q. Jie, Q. Li, Z. Chen, and B. Li, Physica B: Condensed Matter **406**, 52 (2011).

[39] M. Jacobsen, W. Liu, and B. Li, Journal of Physics and Chemistry of Solids **75**, 1017 (2014).